A Novel 2D Piezo-Nanopositioning Stage Based on Triangle Amplifier Mechanism

Liu Xuerui, *Huang Weiqing* *, *Sun Mengxin*

State Key Laboratory of Mechanics and Control of Mechanical Structures,
Nanjing University of Aeronautics and Astronautics, Nanjing 210016, P. R. China

(Received 25 May 2016; revised 17 September 2016; accepted 19 September 2016)

Abstract: To satisfy the demand on dynamic performance and load characteristics of piezoelectric actuators in aeronautics and astronautics fields, a novel 2D piezo-nanopositioning stage utilizing a triangle amplifier mechanism is proposed. The stage is driven by piezoelectric rhombic units in both X and Y directions, which is composed of four piezoelectric stacks. Theoretical static model develops the relationships among output force, displacement, static stiffness and the structure parameters of the platform. The experimental results of the prototype show that the output performances in X and Y directions are similar and both of them are within an 8% deviation from the theoretical values. The stroke of the stage reaches 41.6 μm and 42.9 μm in X and Y directions, respectively, and is directly proportional to the amplitude of the input sinusoidal voltage 10 Hz. Moreover, the nano-positioning stage is featured with bidirectional symmetrical output characteristic and millisecond starting characteristic, whose minimum output displacement step is 50 nm.

Key words: triangle amplifier mechanism; flexure hinges; piezoelectric stacks; bidirectional driving

CLC number: TN384 **Document code**: A **Article ID**: 1005-1120(2017)01-0001-08

0 Introduction

Piezo-nanopositioning stages are widely used in precision, ultra-precision machining and measurement, large scale integrated circuit manufacture, MEMS, scanning probe microscope, biological engineering, due to their high resolution and positioning accuracy[1-3]. In general, for nano-positioning systems, the primary motivation of design is to achieve large travel range[4]. However, the output displacement of piezoelectric materials is small, even the piezoelectric ceramics can barely extend 0.1% of its own length (up to tens of micrometers as usual)[5]. In order to obtain larger travel range and implement nanometer level positioning with high resolution, displacement amplifiers are applied. So far, research on micro displacement amplifiers has mainly focused on the mechanisms such as lever-type, bridge-type, trigonometric and buckling amplification mechanisms[6-11]. Ref. [8] proposed a novel honeycomb amplification structure, whose maximum displacement was approximately 410 μm (single piezoelectric actuator's free stroke was 42 μm), the first resonance frequency was 355 Hz. Ref. [11] presented a bridge-type amplifier, whose maximum stroke reached 963 μm (single piezoelectric actuator's free stroke was 80 μm), and its first resonance frequency was 83 Hz. These amplifiers were actuated forward by the piezoelectric ceramics and backward through the deformation of the elastic structure, leading to asymmetry bidirectional output characteristic and low stiffness of the structure. To satisfy the demand on dynamic performance and load characteristics of piezoelectric actuators in the fields of aeronautics and astronautics in 2015, a novel rhombus displacement amplification mechanism is proposed by our team[12], which is driven by four

* Corresponding author, E-mail address: mehwq@nuaa.edu.cn.

How to cite this article: Liu Xuerui, Huang Weiqing, Sun Mengxin. A novel 2D piezo-nanopositioning stage based on triangle amplifier mechanism[J]. Trans. Nanjing Univ. Aero. Astro., 2017, 34(1):1-8.
http://dx.doi.org/10.16356/j.1005-1120.2017.01.001

piezoelectric stacks. This structure has bidirectional symmetric operating performance while amplifying the displacement. Meanwhile, it has good dynamic characteristics due to the compact arrangement.

For 2-dimensional (2D) actuations, flexure mechanisms are generally utilized to guide the motion of the platform[2-3]. Elastic would improve the resolution and smoothen moving motions as well. Because of the difficulties in motion cross coupling, serial combination of motion guide is widely used for driving and controlling independently in two axes[2,8]. In this study, we propose a novel 2D piezoelectric nano-positioning stage, based on the novel rhombus bidirectional displacement amplification mechanism[12]. In the scheme, diamond-shaped laminated piezoelectric ceramics played the role of core drive unit in each direction. Two perpendicular directions of the stage are separately driven, with flexible parallel four-bar mechanism guiding the directions.

1 Principle and Structure

Fig. 1 shows the basic structure of rhombus bidirectional displacement amplification mechanism based on triangle amplifier [12]. Two triangular blocks are stuck to both ends of the piezoelectric ceramic stacks, and four assemblies are distributed at four edges of the rhombus. When the upper two piezoelectric actuators stretch and the lower ones abridge at the same time, the central part will output a forward displacement D_{out}; On the contrary, the central part will output reverse displacement. Owing to the complete symmetry of the structure, the bidirectional output performance of the structure is completely symmetrical.

The 2D piezoelectric nano-positioning stage, as shown in Fig. 2, consists of two orthogonal tandem rhombus displacement amplifiers as drivers, and a flexible parallel four-bar mechanism as a guider. Interior Y-moving section exports displacement in two directions, and exterior X-moving section propelling X and Y moving section in X-direction. By electric spark wire cutting, the

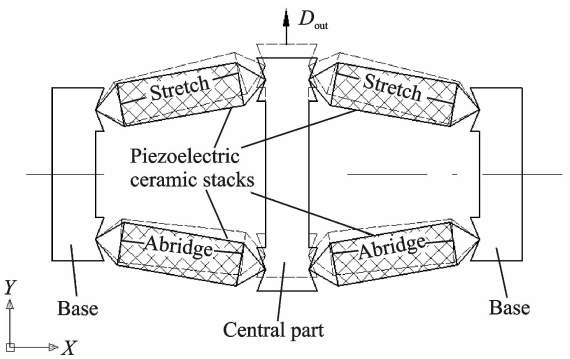

Fig. 1 Rhombus bidirectional displacement amplification mechanism

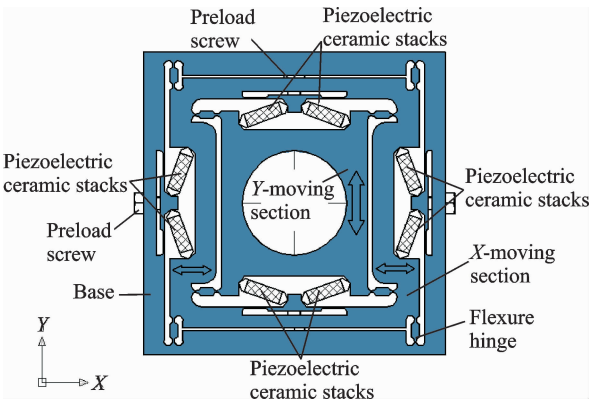

Fig. 2 2D piezoelectric nano-positioning stage

base of the platform processed embeds piezoelectric ceramics units into V-grooves, which is fixed by pre-tightening screw. The 2D piezoelectric nano-positioning stage designed has strong stiffness, relative large displacement and reduced coupling by rhombus bidirectional displacement amplification mechanism and flexible parallel four-bar mechanism. Since the piezoelectric ceramics cannot endure tensile stress[13], the preloaded mechanism is designed to keep the piezoelectric ceramics under compression forces in working status. Fig. 3 shows the preloaded mechanism for

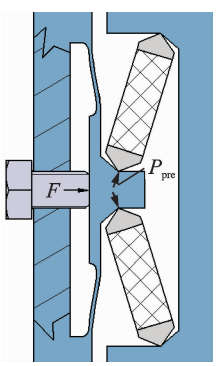

Fig. 3 Preloaded institutions

laminated piezoelectric ceramics in the micro displacement stage.

Thrusted by the preloaded screw (force F), flexible elastic beam promotes a deformation together with the V-grooves and pressurizes two piezoelectric ceramics units at the same time. The pre-tightening force of each piezoelectric ceramics units can be obtained as $P_{\text{pre}}=\dfrac{F}{2\sin\theta}$. Two groups' pre-tightening forces of laminated piezoelectric ceramics are equal in each direction, and the resultant force on Y-moving section is zero.

2 Theoretical Model

Fig. 4 shows a simplified static model of the nano-positioning stage. Piezoelectric ceramic stacks are divided into four groups, named after the voltage of each group. As can be seen in Fig. 4, X and Y directions are controlled by U_1, U_2 and U_3, U_4, respectively. The Y-moving section is entirely nested in the X-moving section. Both directions are guided by the flexible parallel four-bar mechanism. Theoretically, motions in two orthogonal directions are independent.

2.1 Stiffness analysis of flexible hinges

As shown in Fig. 4, flexible hinges are chosen to be the ordinary circular flexure hinges[14-15] in the structure. Supposing that the base of the platform is made of completely linear elastic material, and the rotational stiffness of the straight circular flexure hinge is given by Refs. [14, 16], known as the following expressions

$$K_\alpha=\frac{M_z}{\alpha_z}=\frac{EbR^2}{12\displaystyle\int_{-\frac{\pi}{2}}^{\frac{\pi}{2}}\frac{\cos\omega}{[t/R+2-2\cos\omega]^3}\mathrm{d}\omega} \quad (1)$$

where E is the Young's modulus of circular flexure hinges, R the cutting radius of circular flexible hinges, t the minimum thickness of circular flexible hinges, b the width of the flexible hinges, and h the height of the flexible hinge.

In Fig. 5, when the Y-moving section is forced on the Y direction by $4F_y$, circular flexure hinges will turn a tiny angle α_z round the thinnest place of the flexure hinges. Within the elastic range of the material, we assume that the system is an elastic system. According to energy conservation theorem, the following equation can be obtained.

$$W_F=\frac{1}{2}K_y\delta_y^2=2E_{\text{p1}}+E_{\text{p2}} \quad (2)$$

where $E_{\text{p1}}=\dfrac{1}{2}K_\alpha\alpha_z^2$ is the elastic potential energy of a rotate single flexible hinge as it is in rotation. $E_{\text{p2}}=\dfrac{1}{2}K_s(\delta_y\sin\alpha_z)^2$ is the elastic potential energy of the elastic rod as it is in tension, here, K_s the tensile stiffness of the flexible rod.

The stiffness of a single flexible bar in the Y direction is expressed as

$$K_y=2K_\alpha/l^2+K_s\sin^2\alpha_z \quad (3)$$

It is clear that the stiffness of a single flexible rod in Y direction increases with larger α_z. When α_z is with a small quantity (in the micro displacement stage particularly), the second items in Eq. (3) is a second-order infinitesimal small quantity, which can be ignored. Consequently, given that the stiffness of a single flexible bar in the Y direction can be regarded as a constant, the flexible rod can be regarded as a spring in the Y direction.

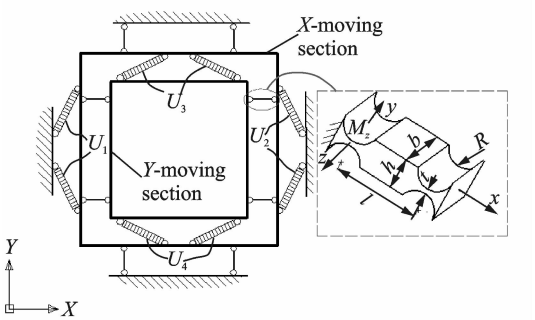

Fig. 4 simplified static model of the nano-positioning stage

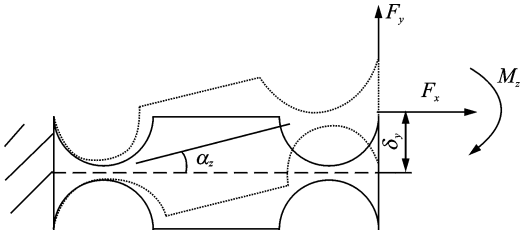

Fig. 5 Force analysis of flexible hinge

2.2 Theoretical static model of the stage

Theoretically, the elongation has a linear relationship with the voltage and the output force of laminated piezoelectric ceramics[13] under a low

frequency. The relationship can be expressed as

$$\delta = nd_{33}U - F/K_a \tag{4}$$

where n is the layer number of laminated piezoelectric, d_{33} the piezoelectric strain coefficient, F the output force of the piezoelectric stacks, and K_a the stiffness of single laminated piezoelectric ceramics.

Thus, we can consider a single laminated piezoelectric ceramic as a spring with stiffness of K_a, when it is preloaded and applied with a constant voltage (e.g. when short-circuited). Accordingly, laminated piezoelectric ceramics in the structure can be predigested as springs at $90° - \theta$ angle with the direction of motion. The force analysis of Y-moving section is shown in Fig. 6.

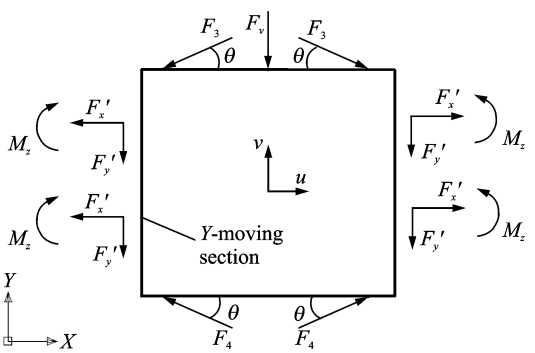

Fig. 6 force analysis of Y-moving section

Considering the Y-moving section as a rigid body, the relationship between output force F and displacement in Y-direction can be simplified as

$$F_v = C_1(U_4 - U_3) - C_2 v \tag{5}$$

where v is the displacement of Y-moving section in the Y direction, constant coefficients are $C_1 = 2nd_{33}K_a\sin\theta$ and $C_2 = 4K_a\sin^2\theta + 4K_y$.

Similarly, supposing that X-moving section is rigid and the tensile stiffness of the flexible rod is strong enough to ignore the displacement of the X-moving section in Y direction, force analysis is similar to that in Y direction. Therefore, the relationship between output forces and output displacement for the stage can be expressed as

$$\begin{bmatrix} F_u \\ F_v \end{bmatrix} = C_1 \begin{bmatrix} U_1 - U_2 \\ U_4 - U_3 \end{bmatrix} - C_2 \begin{bmatrix} u \\ v \end{bmatrix} \tag{6}$$

where F_u, F_v are the forces output in X and Y directions, and u, v are the displacements of Y-moving section in the X and Y directions, respectively.

In Eq. (6), motions in two directions are theoretically independent of each other. Output force and displacement are influenced by the difference between voltages of two piezoelectric stacks groups in the same direction. Thus, for the sake of larger output force and displacement, increasing the difference between voltages is effective. Whereas, for the specified piezoelectric ceramics available, the highest voltage is limited. When the voltages are applied to the piezoelectric ceramics stacks without constraint of external force, the Y-moving section generates the maximum displacement as follows

$$\begin{bmatrix} u_{\max} \\ v_{\max} \end{bmatrix} = \frac{C_1}{C_2} \begin{bmatrix} U_1 - U_2 \\ U_4 - U_3 \end{bmatrix}_{\max} \tag{7}$$

When the stage is constrained by external force without output displacement, it can produce the maximum force as

$$\begin{bmatrix} F_{u\max} \\ F_{v\max} \end{bmatrix} = C_1 \begin{bmatrix} U_1 - U_2 \\ U_4 - U_3 \end{bmatrix}_{\max} \tag{8}$$

Furthermore, when all of the piezoelectric ceramics stacks of the stage are preloaded and applied a constant voltage, the Y-moving section can be simplified as an elastic structure with static stiffness of C_2 in two directions. In conclusion, the coefficients C_1 and C_2 determine the static mechanical properties of the stage in the design process. From Eq. (5) in each direction, the stiffness C_2 is composed of the stiffness of the parallel four-bar mechanism and the laminated piezoelectric ceramics.

Static theoretical analysis and modeling helps us select and optimize the structural parameters. Coefficient C_1 and C_2 are the functions of parameters of laminated piezoelectric ceramics, flexible hinges and the angle θ. Therefore, when the laminated piezoelectric ceramics are selected, structural parameters are determined by the desired output performance.

3 Experiment and Results

According to the theoretical modeling, the parameters of micro displacement stage are deter-

mined in Table 1, and the prototype of the nano-positioning stage with four groups of piezoelectric ceramics units is shown in Fig. 7. Here, the piezoelectric ceramics from the Danish company NOLIAC (NAC2013-H14) is selected; whose base and triangular blocks are made of 65Mn spring steel. The structure of the base is processed by electric spark wire cutting, ensuring the maximum machining accuracy and the symmetry of the structure.

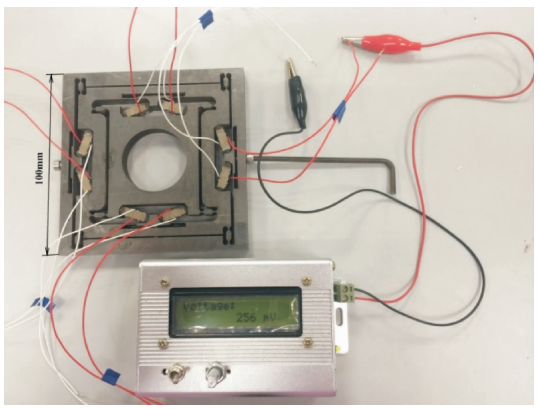

Fig. 7 Prototype of nano-positioning stage and assembly

Charge amplifier in Fig. 7 is used to assemble, which has been calibrated the linear relationship between the charge (display as voltage on the screen) and the pre-tightening force. Each of piezoelectric ceramics stacks is pre-loaded with the optimal force of 50 N.

Table 1 Geometric size and material parameters

Parameter		Value
Geometric parameter	R/mm	1.75
	t/mm	0.5
	b/mm	10
	h/mm	4
	l/mm	8
	θ/(°)	20
Parameter of piezoelectric stacks	K_a(measured)/(N·μm^{-1})	10
	δ_{max}(150 V)/μm	19.8
Parameter of 65Mn	E/GPa	210
	σ_s/MPa	⩾784

Fig. 8 shows the experimental setup of the prototype. The 2D nano-positioning stage is fixed on the vibration isolation table. Laser displacement sensor (KEYENCE Inc. LK-H1W) measures the output displacements. Stiffness of the

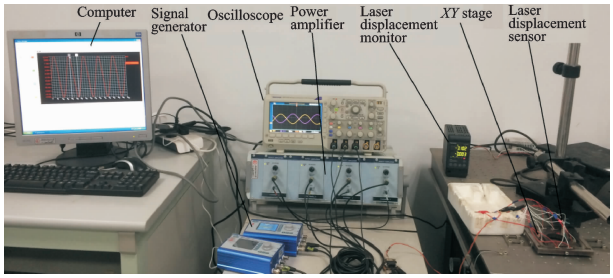

Fig. 8 Experimental setup

stage with or without piezoelectric ceramics units is obtained by balancing weight. The signal generator generates positive input voltage (U_1, U_2, U_3 and U_4). According to Eq. (6), the output displacement of the stage is in a linear correlation with the difference between voltages of two piezoelectric ceramics groups in one direction (U_1-U_2, U_4-U_3). Therefore, we consider the voltage difference as the control signal.

Table 2 shows the comparison between specific measurement results and theoretical values. The errors between theoretical and measuremental results in the X direction are larger than thaose in the Y direction, and it is probably owing to the simplified theoretical model of force transmission structure in the X direction. Theoretical maximum output displacement of the stage is approximately 44.4 μm in both X and Y directions. Strokes measured in the experiment are 41.6 μm and 42.9 μm in X and Y directions, as shown in Fig. 9, which approaches to the theoretical stroke. When the stage is powered in one direction, it generates coupled displacement (no more than 11.7% of the maximum stroke) in the other direction, errors might be caused by inadequate machining accuracy. However, full symmetry can hardly be guaranteed under actual processing condition. Thus, forces output by each piezoelectric ceramics units are non-uniform, which leads to the coupled displacement.

Measured stiffness of flexure hinges in the actuation direction ($4K_y$) is larger than the theoretical value, which is mainly because of the surface residual stress produced during the electric spark wire cutting process. Experimental stiffness of the structure with piezoelectric ceramics

units embedded in it approaches to the theoretical calculation values (errors within 7.9%) in one direction. It proves that the stiffness in one direction is composed of stiffness of the parallel four-bar mechanism and two groups of laminated piezoelectric ceramics. Accordingly, we consider the theoretical model reasonable and useful for designing and optimizing the stage structure.

Table 2 Theoretical and experimental results

Parameter		Stroke/μm	Coupled displacement/μm	Stiffness of flexure hinges $4K_y$/(N·μm^{-1})	Total stiffness/(N·μm^{-1})
X-direction	Theoretical value	44.4	0	2.576	7.255
	Experimental value	41.6	4.85	2.711	7.874
	Error/%	6.7	—	5.0	7.9
Y-direction	Theoretical value	44.4	0	2.576	7.255
	Experimental value	42.9	3.524	2.693	7.619
	Error/%	3.5	—	4.3	4.8

Fig. 9 shows the hysteresis loops of the output displacement in two directions when voltages applied to the prototype are from 0 to 180 V. The shapes of the hysteresis loops in two directions are similar. The maximum width ratios of the hysteresis loops are 9.4% in the X direction and 10.2% in the Y direction. At the same time, the hysteresis loops are centro-symmetric, which means the bidirectional output performances of the nano-positioning stage are symmetrical in two directions.

Fig. 10 shows the relationships between the amplitude of the output displacement and the input sinusoidal control signal, where the amplitude of the sinusoidal voltage at 10 Hz raises from 10 V to 200 V in two directions. The output performances in two directions are similar. The linear goodness-of-fit reach 99.68% and 99.77% in X and Y directions, respectively, indicating its good linearity. The linear fit of the relationships proves that the output displacement is proportional to input voltage.

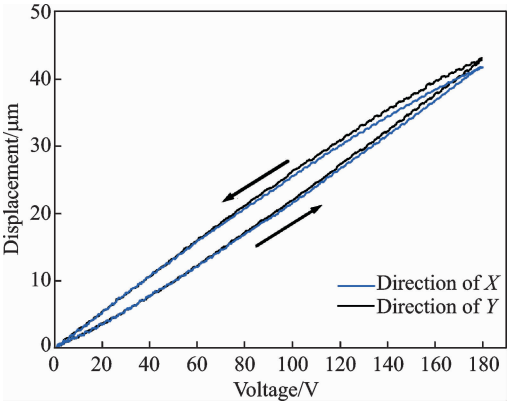

Fig. 9 Hysteresis loops of Y-moving section in X and Y directions

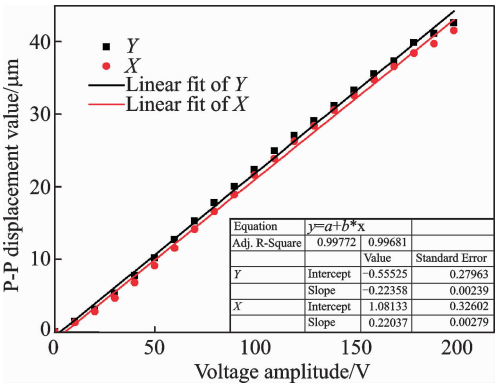

Fig. 10 Relationship between amplitudes of output displacement and input control signal under sinusoidal voltage of 10 Hz

As shown in Fig. 11, under open loop control, the minimum output displacement step of the stage in the X, Y directions is 50 nm. Through signal generator, the step of the staircase voltage increases stepwise: keep the amplitude of the staircase voltage stepping from 0.05 V to higher. The laser displacement sensor measures the output displacements in the two directions. When the step amplitude of voltage is 0.25 V, the steps of output displacement in two directions are relatively stable.

Fig. 12 shows the step response of the Y-moving section in the Y direction under different amplitude of the step voltage with an open loop control.

The Y-moving section weighs 148 g (calculation value). By the linear fitting of the rising curve part, we can obtain the response speeds under different amplitudes of the step voltage (from

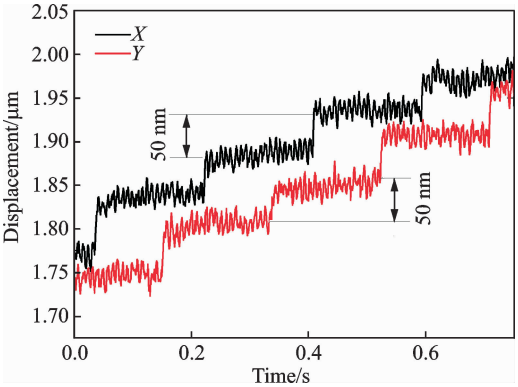

Fig. 11 The minimum output displacement step of nano-positioning stage in X, Y directions

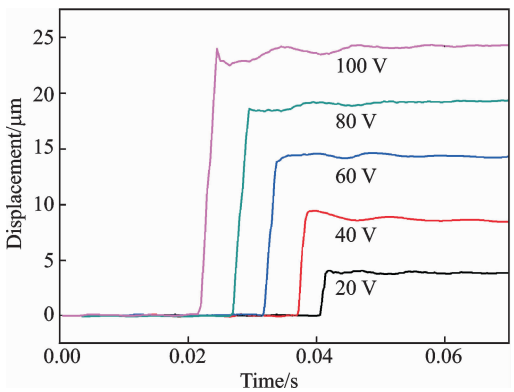

Fig. 12 Step response of Y-moving section in Y direction

20 V to 100 V). The speeds are 3.868, 7.886, 7.062, 7.158 and 8.945 mm/s; and the time to peak are 0.001 5, 0.001 3, 0.002 3, 0.002 7 and 0.002 7 s, respectively. Accordingly, we consider that the response time of the stage is in milliseconds, which means a rapid response speed. Meanwhile, the stabilization time is less than 0.02 s. In a word, the stage has millisecond starting characteristic, which can achieve the speedy response and positioning.

4 Conclusions

A novel 2D piezoelectric nano-positioning stage is proposed based on triangle amplifier mechanism, which is driven by innovative piezoelectric rhombic units and guided by the flexible parallel four-bar mechanism in both actuating directions. Two rhombus displacement amplifiers are vertical and independent of each other, as Y-moving section is entirely nested in the X-moving section. This design improves the dynamic and bidirectional performances of traditional nano-positioning actuators.

Theoretical statics model of the nano-positioning stage is built to select and optimize the structural parameters. Relationship among output force, displacement, static stiffness and structural parameters is presented. Meanwhile, it is discovered that the total stiffness is composed of that of the parallel four-bar mechanism and the laminated piezoelectric ceramics in one direction.

According to the theoretical modeling, prototype experiment was conducted. The stroke of the stage measured reaches 41.6 μm and 42.9 μm in the X and Y directions, respectively. The total static stiffness tested in one direction has an error within 8% deviation from the theoretical one, which verifies the theoretical model. When the stage is powered in only one direction, the other one generates coupled displacement (less than 11.7% of the maximum stroke), and that is probably because of the asymmetry of the structure produced during the machining process. The shapes of the hysteresis loops in two directions are similar, i. e. centrosymmetric, which means that the bidirectional output performances of the stage are symmetrical. Under the sinusoidal voltage of 10 Hz, output stroke is directly proportional to the amplitude of the input voltage with a good linearity. The nano-positioning stage has the minimum output displacement step of 50 nm and the millisecond starting characteristic. Although the micro displacement platform has small stroke compared with traditional displacement amplifiers, it can output symmetrical bidirectional performances with great dynamic characteristics, which could be further applied to rapid precision positioning technology and optical precision engineering.

Acknowledgements

This work was supported partly by the Project on Integration of Industry, Education and Research of China Aviation Industry Corp. (No. CXY2013NH09), the National Natural Science Foundation of China (No. 51375224). The authors would like to acknowledge the following professors and students for their assistance: Prof.

Huang Weiqing, Sun Mengxin, Su Zhao, Dang Bingnan, and Wang Yin, all from the State Key Laboratory of Mechanics and Control of Mechanical Structures, Nanjing University of Aeronautics and Astronautics.

References:

[1] GUO Z, TIAN Y, LIU C, et al. Design and control methodology of a 3-DOF flexure-based mechanism for micro/nano-positioning[J]. Robotics and Computer-Integrated Manufacturing, 2015, 32: 93-105.

[2] CHEN W H, WANG Y X, SHEN X, et al. Neural network PID real-time control for active vibration reduction using piezoceramics stacks[J]. Journal of Nanjing University of Aeronautics & Astronautics, 2014,46(4):587-593. (in Chinese)

[3] SHIMIZU Y, PENG Y, KANEKO J, et al. Design and construction of the motion mechanism of an XY micro-stage for precision positioning[J]. Sensors and Actuators A: Physical, 2013, 201: 395-406.

[4] CHEN M, TZENG H. Implementation of a novel large moving range submicrometer positioner[J]. Mechatronics, 2009, 19(7): 1143-1151.

[5] UCHINO K. Ceramic actuators: Principles and applications[J]. MRS Bulletin, 2013(4): 42-48.

[6] CHEN J, ZHANG C, XU M, et al. Rhombic micro-displacement amplifier for piezoelectric actuator and its linear and hybrid model[J]. Mechanical Systems and Signal Processing, 2015(50/51): 580-593.

[7] LIN C. Structural design and control strategy analysis of micro/nano transmission platform[J]. Transactions of Nanjing University of Aeronautics and Astronautics,2014,31(5):484-491.

[8] MURAOKA M, SANADA S. Displacement amplifier for piezoelectric actuator based on honeycomb link mechanism[J]. Sensors and Actuators A: Physical, 2010, 157(1): 84-90.

[9] CALLOW D, LEE J, BLUMENSTEIN M, et al. Development of hybrid optimisation method for artificial intelligence based bridge deterioration model — Feasibility study[J]. Automation in Construction, 2013, 31: 83-91.

[10] LAM K H, WAN X X, CHAN H L W. Lead-free piezoceramic cymbal actuator[J]. Sensors and Actuators A: Physical,2006, 125(2): 393-397.

[11] CHIANG M, CHEN C, TSOU T. Large stroke and high precision pneumatic-piezoelectric hybrid positioning control using adaptive discrete variable structure control[J]. Mechatronics,2005, 15(5): 523-545.

[12] HUANG W Q, SHI X Q, WANG Y. Design of diamond piezoelectric micro displacement amplification mechanism[J]. Opt Precision Eng, 2015, 23(3): 803-809. (in Chinese)

[13] PREUMONT A. Piezoelectric systems[M]. 1st Edition. Berlin: Springer Netherlands, 2006(136): 95-130.

[14] YONG Y K, LU T F, HANDLLEY D C. Review of circular flexure hinge design equations and derivation of empirical formulations[J]. Precision Engineering, 2008, 32(2): 63-70.

[15] FRIEDRICH R, LAMMERING R, HEURICH T. Nonlinear modeling of compliant mechanisms incorporating circular flexure hinges with finite beam elements[J]. Precision Engineering, 2015, 42: 73-79.

[16] PAROS J M W L. How to design flexure hinges[J]. Machine Design,1965, 27(37): 151-157.

Ms. **Liu Xuerui** received her B. S. degree in Aircraft Design and Engineering from Nanjing University of Aeronautics and Astronautics in 2014. Her research focuses on the piezoelectric precision drive technology.

Prof. **Huang Weiqing** received his Ph. D. degree in Mechanical Engineering from Hong Kong University of Science and Technology in 1999. His research focuses on the piezoelectric precision drive and control technology.

Mr. **Sun Mengxin** received his B. S. degree in Aircraft Design and Engineering from Nanjing University of Aeronautics and Astronautics in 2012, and is currently a Ph. D. candidate at Nanjing University of Aeronautics and Astronautics. His research focuses on the piezoelectric precision drive and control technology.

(Executive Editor: Zhang Tong)